

## NANOCOMPOSITES OF POLY(LACTIC ACID) REINFORCED WITH CELLULOSE NANOFIBRILS

Ping Qu, Yuan Gao, Guo-feng Wu, and Li-ping Zhang \*

A chemo-mechanical method was used to prepare cellulose nanofibrils dispersed uniformly in an organic solvent. Poly(ethylene glycol) (PEG 1000) was added to the matrix as a compatibilizer to improve the interfacial interaction between the hydrophobic poly(lactic acid) (PLA) and the hydrophilic cellulose nanofibrils. The composites obtained by solvent casting methods from N,N-Dimethylacetamide (DMAc) were characterized by tensile testing machine, atomic force microscope (AFM), scanning electron microscope (SEM), and Fourier transform infrared spectroscopy (FT-IR). The tensile test results indicated that, by adding PEG to the PLA and the cellulose nanofibrils matrix, the tensile strength and the elongation rate increased by 56.7% and 60%, respectively, compared with the PLA/cellulose nanofibrils composites. The FT-IR analysis successfully showed that PEG improved the intermolecular interaction, which is based on the existence of intermolecular hydrogen bonding among PLA, PEG, and cellulose nanofibrils.

*Keywords:* Cellulose nanofibrils; Poly(lactic acid); Interfacial interaction; Nanocomposites

*Contact information:* College of Material Science and Technology, Beijing Forestry University, Beijing, 100083, PR China; \* Corresponding author: zhanglp418@163.com

### INTRODUCTION

In order to help reduce environmental pollution caused by petroleum-based products, decrease the dependence on nonrenewable resources, and maintain the CO<sub>2</sub> balance, material scientists and engineers have developed biobased material with controlled properties (Mangiacapra et al. 2005; Yang et al. 2006; Gupta and Revagade 2007; Marras et al. 2007). Poly(lactic acid) (PLA) is a type of commercial biopolymer made from L- and D-lactic acids, which can be derived from the fermentation of corn starch (Lunt 1998). The use of such bio-based materials can help maintain the balance of carbon in nature. In comparison with traditional plastics, PLA has good mechanical properties. However, it still has deficiencies such as brittleness, low impact strength, and low ability in resisting thermal deformation, which limit the extensive application of pure PLA (Wu 2008).

Cellulose, the world's most abundant natural, renewable, and biodegradable polymer (Azizi et al. 2005; Nada et al. 2009), can be found in plants such as grasses, reeds, stalk, woody vegetation, bacteria, and some amoebas. Cellulose is a polydisperse linear polymer of poly-(1, 4)-D-glucose residues. The monomers are linked together by condensation, such that the sugar rings are joined by glycosidic oxygen bridges. Cellulose consists of crystalline phases and amorphous phases at a nanometer level, which are

bonded by intra- and inter-molecular hydrogen bonds and van der Waals forces that maintain the self-assembled macromolecular structure and the fibril morphology. Cellulose nanofibrils can be obtained through chemical (Beck-Candanedo et al. 2005; Bondeson et al. 2006; Gray and Roman 2006), physical (Takahashi et al. 2005), or biological processes (Asako et al. 1997). Geometrical characteristics of cellulose nanofibrils depend on both the origin of cellulose nanofibrils and the processing conditions such as time, temperature, and purity of materials.

In natural structures, cellulose nanofibrils already act as reinforcing elements. Cellulose nanofibrils consist of slender parallelepiped rods with lateral dimension at the nanometer level, high aspect ratio, and relatively large surface areas, and they also have a renewable character (Megan et al. 2004). The tensile modulus of a single whisker has been found to be 143 GPa (Sturcova et al. 2005). Cellulose nanofibrils have been mainly employed as fillers in several kinds of polymeric matrixes from aqueous suspension, giving rise to a very strong and tough percolating networks of hydrogen-bonded nanofibrils (Favier et al. 1995; Dubief et al. 1999; Dufresne 2000; Angles and Dufresne 2001; Samir et al. 2004).

When using nanofibrils with commonly used matrix polymers, the poor compatibility related to the interfacial adhesion between the hydrophilic cellulose nanofibrils and the hydrophobic matrix can hinder the nanofibrils from dispersing well in the matrix (Lu et al. 2008). At present, chemical grafting onto the cellulose nanofibrils has been carried out to improve the compatibility between the cellulose nanofibrils and the matrix. However, the mechanical performances of the resulting composites are not as high as expected, which is possibly due to destruction of the crystal structure of cellulose. Also, the surface modification of cellulose nanofibrils will affect the degradation rate (Heux et al. 2000; Gousse et al. 2002; Oksman et al. 2006; Petersson et al. 2007; Dai and Kadla, 2009). Cellulose nanofibrils/PLA nanocomposites prepared by melt compounding technique was reported by Oksman et al. (2006), but the sample color changed from transparent yellow to light brown, which indicated thermal degradation of the cellulose nanofibrils and the PLA.

In this paper, we report the use of a new method to make the cellulose nanofibrils disperse homogeneously in an organic solvent in preparation for composite formation. In addition, a solution-casting method, which can avoid the degradation, was used to produce the nanocomposites. However, the poor compatibility of between the hydrophobic PLA and the hydrophilic cellulose nanofibrils in the composite was a great challenge, which was settled by adding PEG to the matrix as a compatibilizer.

Besides the usage of modified PLA in packaging, the nanocomposites can be a potential tissue engineering implant in the clinical application because of better biocompatibility. The abundant exposed hydroxyl (-OH) groups afford the nanocomposites a good water absorbing ability and contribute to their biodegradability. The degradation rate also can be controlled by addition varying amounts of cellulose nanofibrils. The nanocomposites were thoroughly characterized by atomic force microscopy (AFM), scanning electron microscopy (SEM), Fourier transform infrared spectroscopy (FT-IR), and tensile testing.

## EXPERIMENTAL

### Materials

Bleached wood pulpboard (sulfate cooking) was purchased from a pulp and paper mill in Shandong province, China. Poly(lactic acid) (PLA, Mw=100,000, purchased from Shanghai Yisheng industry Ltd.) was used as the matrix. The additive was poly(ethylene glycol) (PEG 1000). The solvents N,N-dimethylacetamide (DMAc) and sulfuric acid (98%) were purchased from Shantou Xilong Chemical Plant and Beijing Chemical Plant, respectively.

### Preparation of Nanocomposites

#### *Preparation of suspension of cellulose nanofibrils in organic solvent*

After the pretreatment of the pulpboard in diluted sulfuric acid (15 %) at a constant mixing speed of 200 rpm for 4 hour at 80 °C (at a solid to liquid ratio of 1:20), the suspension was vacuum filtered, and the cake was washed first with deionized water to remove the H<sup>+</sup> and SO<sub>4</sub><sup>2-</sup>, then washed with DMAc to remove the water in it. After that, the cake was immersed into DMAc, and the pretreated cellulose was suspended in the DMAc, which was then homogenized at a high pressure of 100 MPa for 10 times (GEA Niro Soavi, Italy). Through the combination of pretreatment and homogenization, the cellulose nanofibrils became well dispersed in DMAc.

#### *Preparation of PLA*

A 16 wt% solution of PLA in DMAc was prepared by stirring the solution in a water bath at 70 °C. The PLA was scraped with a scraper on glass and then dried on an electric heating board at 80 °C. After that, the obtained PLA (50 μm) was placed under vacuum condition at 40 °C for 24 h to ensure that the solvent had completely evaporated.

#### *Preparation of PLA/cellulose nanofibrils composites*

First, the cellulose nanofibrils (3 wt% based on polymer content) were dispersed in DMAc to form a suspension. Then, PLA was added into the suspension at 70 °C with agitation in an ultrasonic bath for 2 h. (KQ5200DB, China). The composites were scraped with a scraper on glass and then dried on an electric heating board at 80 °C. After that, the obtained composites (50 μm) were placed under vacuum condition at 40 °C for 24 h to ensure that the solvent had completely evaporated.

#### *Preparation of PLA/cellulose nanofibrils/PEG composites*

PEG (2 wt% based on polymer content) and PLA were added to the cellulose nanofibrils suspension (3 wt% based on polymer content) simultaneously. The composites were scraped with a scraper on glass and then dried on an electric heating board at 80 °C. After that, the obtained composites (50 μm) were placed under vacuum condition at 40 °C for 24 h to ensure that the solvent had completely evaporated.

## Performance and Characterization of Nanocomposites

### *Tensile testing*

A tensile testing machine (DCP-KZ300) was used to measure the tensile strength at the point of breakage of each composite. Testing was conducted at a crosshead speed of 20 mm/min using thin plates (50  $\mu\text{m}$ ). Five measurements were made for each composite, and the data averaged to obtain a mean value. The samples were cut into pieces with a width of 15 mm and a total length of 100 mm.

### *Atomic force microscope (AFM)*

The cellulose nanofibrils, as well as the nanocomposites, were characterized using a SHIMADZU SPn9000 scanning probe microscope. Images were collected using a phase mode with a constant force. For the analysis of cellulose nanofibrils, a droplet of the DMAc suspension of 1% cellulose nanofibrils was dried on a mica surface prior to AFM examination. The nanocomposites were analyzed directly.

### *Scanning electron microscope (SEM)*

The fracture surfaces of pure PLA, PLA/cellulose nanofibrils, and PLA/cellulose nanofibrils/PEG composites were studied with a JSM5900 scanning electron microscope (SEM) under an accelerating voltage of 5 kV. Prior to the SEM examination, samples were broken to expose the internal structure for SEM studies, and all the surfaces were sputtered with gold.

### *FT-IR characterization*

FT-IR spectra of the native cellulose were obtained with dried powdered samples on a Tensor 27 (Bruker, Germany) device in the range of 4,000-600  $\text{cm}^{-1}$ . Pellets were prepared from the mixtures of the samples and KBr (1:100 in weight). 32 scans were accumulated at a resolution of 2  $\text{cm}^{-1}$ . In order to investigate functional groups and the structure of the nanocomposites, the FT-IR technique was used within a frequency range of 4000-600  $\text{cm}^{-1}$ . The thickness of the composites was prepared in the range of 10-20  $\mu\text{m}$ .

## RESULTS AND DISCUSSION

### **Structure of Cellulose Nanofibrils**

The structure of the cellulose nanofibrils obtained was analyzed through AFM, and it was found to be affected by many factors such as acid concentration, acid treatment time and temperature, working pressure, and times of the homogenization. The dimension of the cellulose nanofibrils was about 50 nm in width and several micrometers in length (Fig. 1.).

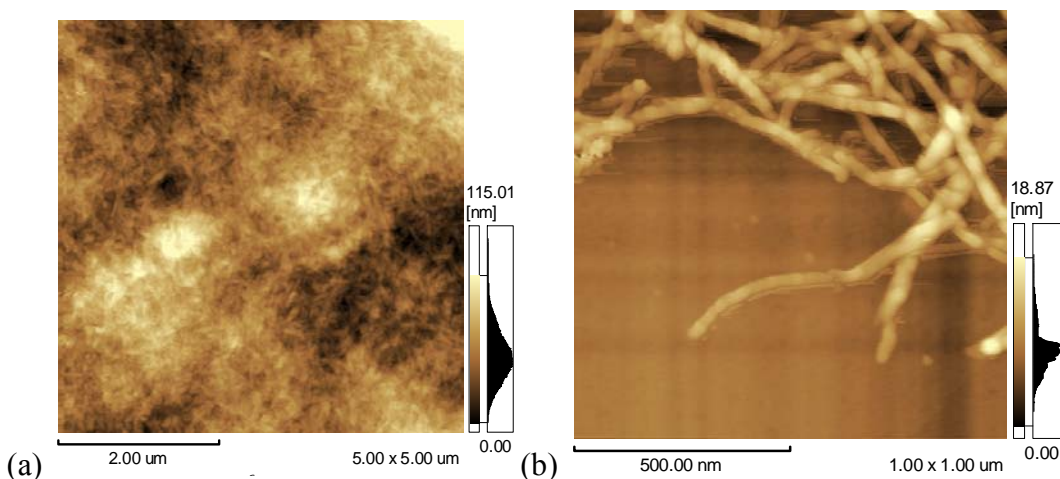


**Fig. 1.** The structure of the produced nanofibrils analyzed with AFM. (a) an overview of the cellulose nanofibrils, (b) a detailed view of the cellulose nanofibrils

### Mechanical Properties of Nanocomposites

The results of mechanical test are presented in Fig. 2. The figure shows the effects of cellulose nanofibrils and dispersants (PEG) on the tensile strength and elongation compared with pure PLA. After adding cellulose nanofibrils to the PLA matrix, its tensile strength was 30 MPa and elongation was 2.5 %. Compared with the pure PLA, its mechanical properties decreased. This finding is attributed to poor interfacial bonding between the cellulose nanofibrils and the PLA matrix. And the existence of the cellulose nanofibrils, as an obstruction, separates the molecular chains of PLA, which makes the distance among the molecules larger and the force among the molecular chains of PLA weaker. The interaction between PLA and cellulose nanofibrils was too weak to counteract the loading. However, when the PEG was added to the blend of PLA and cellulose nanofibrils, the composites showed significant improvements in tensile strength and elongation. The tensile strength and the elongation increased by 28.2% and 25%, respectively, compared with pure PLA, and increased by 56.7% and 60% compared with the PLA/cellulose nanofibrils. It is clear that the addition of PEG had a positive effect on the composites, increasing the strength of the composites. PEG, acting as a kind of compatibilizer, successfully improved the interaction between the hydrophobic PLA and the hydrophilic cellulose nanofibrils.

The reason might be that PEG covers the surface of the cellulose nanofibrils. PEG is expected to act not only as a plasticizer for PLA to improve its elongation, but also as a compatibilizer between the hydrophobic PLA and the hydrophilic cellulose nanofibrils. PEG also prevents the aggregation of the nanofibrils, so the cellulose nanofibrils dispersing in the PLA matrix homogeneously form a network structure to reinforce the PLA.

Figure 3 shows the tensile strength and elongation at break of the composites with different cellulose contents. Results obtained from the mechanical properties show that both tensile strength and elongation at break reached a maximum when the content of cellulose nanofibril was 3%, and decreased with further increase of cellulose nanofibrils. This may be attributed to the increased aggregation among cellulose nanofibrils.

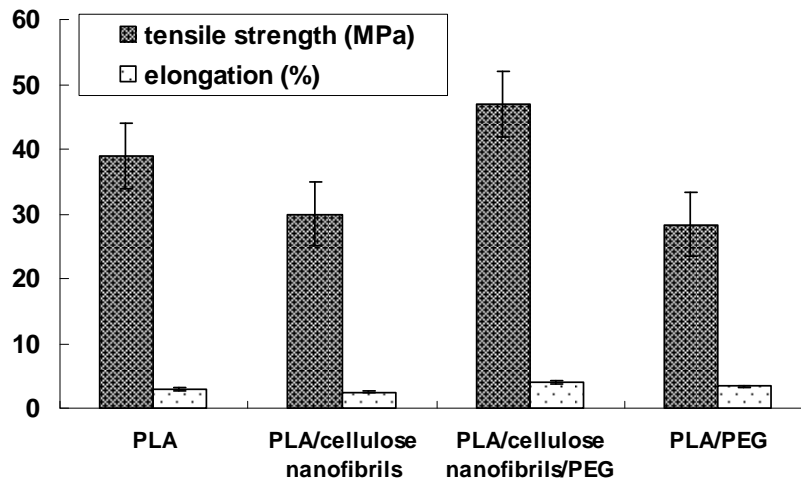


Fig. 2. Tensile strength and elongation of the different kinds of composites

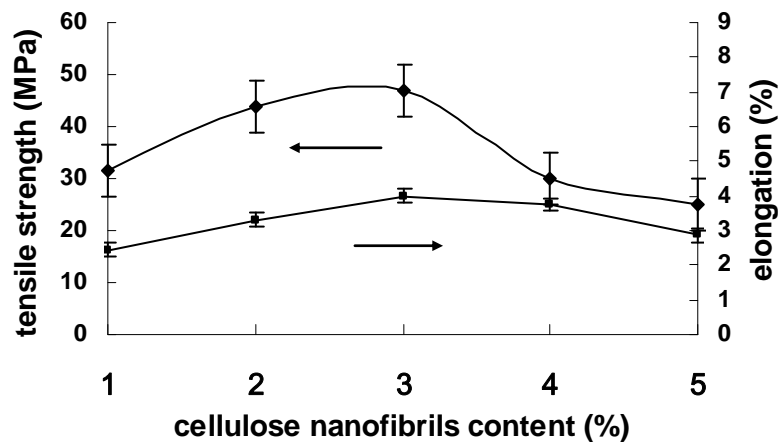
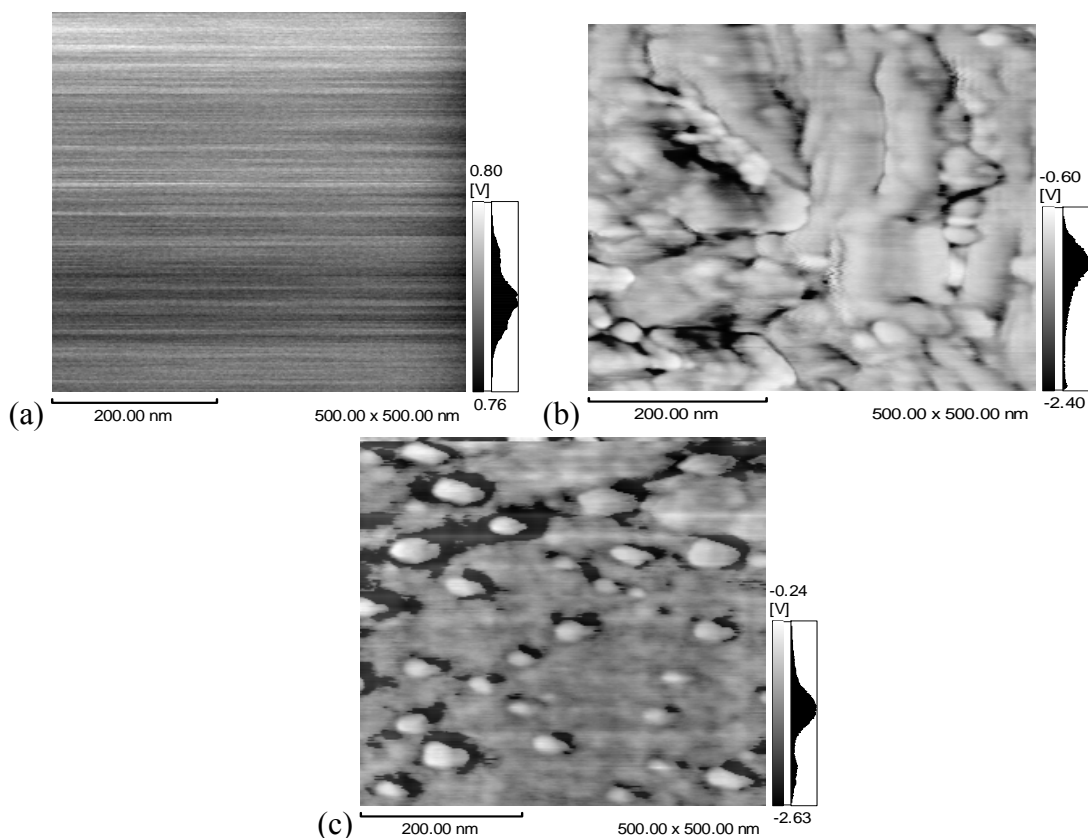


Fig. 3 Different cellulose nanofibrils content on mechanical properties of the composites

### Morphology of Nanocomposites

It is necessary to study the morphology of the composites, since their mechanical properties depend on it (Wu and Liao 2005). The morphology of the pure PLA surface is relatively flat, which is shown in Fig. 4a. From Fig. 4b, the cellulose nanofibrils are relatively homogeneously distributed in the PLA matrix and are wrapped by molecular chains of PLA. However interspaces between the PLA and the cellulose nanofibrils are readily apparent. The picture of the PLA/cellulose nanofibrils/PEG composites is given in Fig. 4c. The interspaces are not apparent in this case, and only part of the cellulose nanofibrils are exposed on the surface. The cellulose nanofibrils and the PLA matrix form a sea-island structure.



**Fig. 4.** The surface morphologies of the pure PLA (a), the PLA/cellulose nanofibrils (b), and PLA/cellulose nanofibrils/PEG composites (c) by atomic force microscope

The mechanical performance of composites is dependent not only on the degree of dispersion of the fibers in the polymer matrix, but also on the nature and intensity of fiber–polymer adhesion interactions (Salmi et al. 2009; Thomas et al. 2009). It can be seen that the cellulose nanofibrils were dispersed homogeneously in the matrix, and the interface between the cellulose nanofibrils and the PLA matrix was effectively improved. The results showed that the PEG, as a good compatibilizer, was able to effectively reinforce the interfacial action and miscibility between PLA and cellulose nanofibrils. The materials could transfer the stress and improve the tensile strength because of the good compatibility on the interface, which was in agreement with the mechanical results. Hydrogen bonds were able to form between PLA and cellulose nanofibrils due to the existence of the PEG. The interactive forces including van der Waals force (dipole–dipole and dispersion forces), electrostatic forces, and polar forces among the PLA, cellulose nanofibrils, and PEG increased markedly.

### Fracture Surfaces of Nanocomposites

SEM photos show the fracture surface morphology of the pure PLA, the PLA/cellulose nanofibrils composites, and the PLA/cellulose nanofibrils/PEG. Relatively smooth fractures can be seen in Fig. 5a. The pure PLA is prone to brittle fracture in which molecules are detached neatly.

After cellulose nanofibrils were added into PLA, the cross section showed irregular protrusions and holes. Compared with the SEM micrograph of PLA/cellulose nanofibrils and PLA/cellulose nanofibrils/PEG composites, it can be seen that the surface of the PLA/cellulose nanofibrils/PEG had more holes and threadlike structure. The fracture surfaces of the two kinds of composites were completely different. In Fig. 5b, the surface morphology is different from Fig. 5c. Therefore, it can be concluded that the PEG is a good compatibilizer for PLA and cellulose nanofibrils. With the addition of the cellulose nanofibrils and the PEG to the PLA matrix, the fracture section became more and more uneven due to the interfacial adhesive force. The results show trends similar to those of the mechanical properties of the composites; the more irregular of the fracture surface, the better were the mechanical properties (Singha and Thakur 2009).

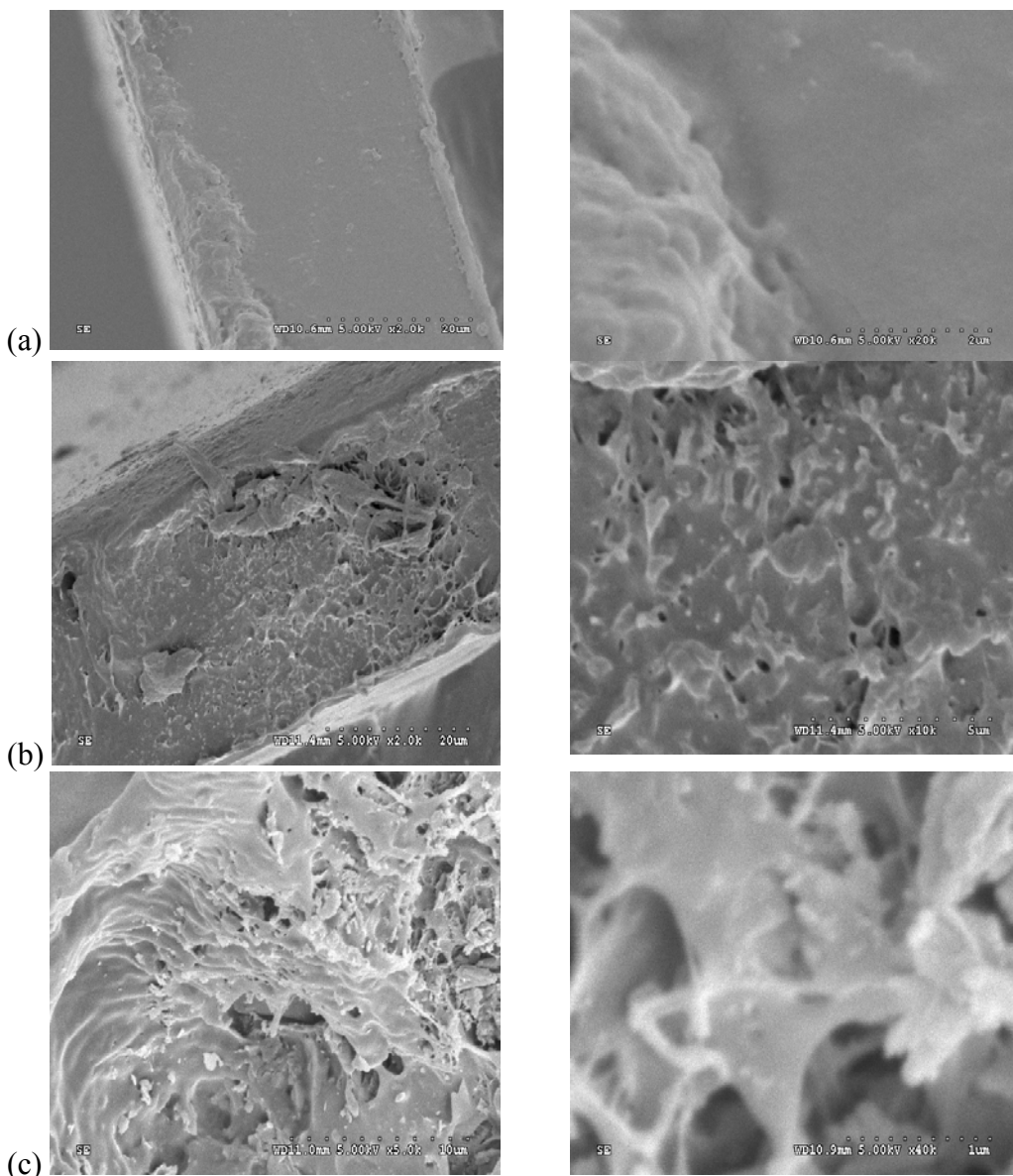


**Fig. 5.** SEM micrographs of fracture surfaces of pure PLA (a); PLA/cellulose nanofibrils (b); PLA/cellulose nanofibrils/PEG (c)

### FT-IR Characterization of Nanocomposites

The interaction of polymer composites can be identified by means of FT-IR spectra. If two polymers form completely immiscible blends, then there are no appreciable changes in the FT-IR spectra compared with those of each component (Zhang et al. 2003). However, if two polymers are compatible, a distinct chemical interaction (a hydrogen bonding or dipolar interaction) exists between their chains, causing the IR spectra of the composites to change (e.g., band shifting and broadening) (Peng et al. 2005). As a result, FT-IR can identify segment interactions and provide information about the phase behavior of polymer composites. The results indicated that hydrogen bonds form among hydroxy groups of the cellulose surfaces and the terminal hydroxyl, terminal carboxyl, and carbonyl groups of PLA.

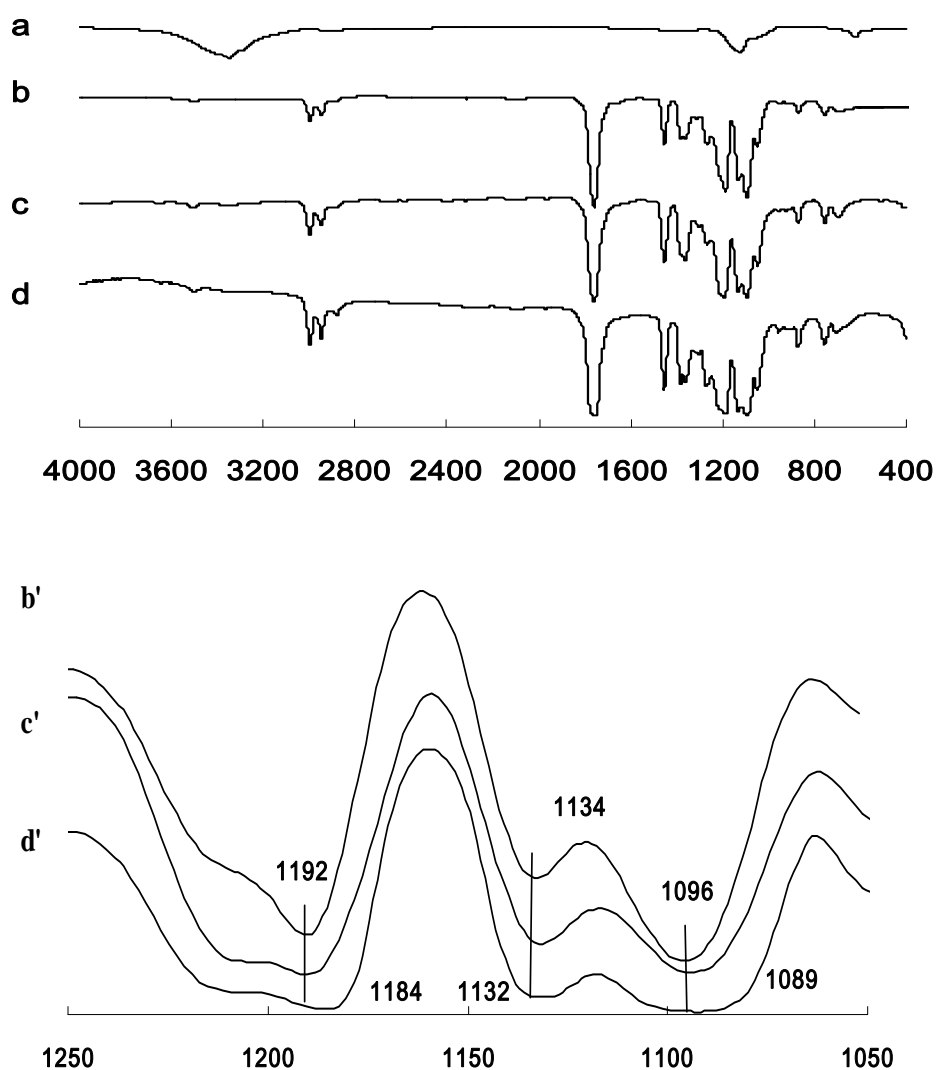


**Fig. 6.** FT-IR of cellulose nanofibrils (a), pure PLA membrane (b), PLA/cellulose nanofibrils composites (c), PLA/cellulose nanofibrils/PEG composites (d), and the spectra of wavenumbers between 1250-1050 cm<sup>-1</sup> were magnified as showed in (b'), (c') and (d')

Figure 6 shows the spectra of cellulose nanofibrils (a), pure PLA membrane (b), PLA/cellulose nanofibrils composites (c), and PLA/cellulose nanofibrils/PEG composites (d). From the spectrum of (a), it can be observed that the hydrogen bonded -OH stretching was located at  $3347\text{ cm}^{-1}$ , the C-H stretching at  $2903\text{ cm}^{-1}$ , the -CH<sub>2</sub> bending situates at  $1429\text{ cm}^{-1}$ , and the C-H bending at  $1370\text{ cm}^{-1}$ , which represent characteristic peaks of cellulose nanofibrils. The peak at  $1058\text{ cm}^{-1}$  is related to the C-O stretching. The C-H bending and -CH<sub>2</sub> stretching at  $899\text{ cm}^{-1}$  indicate the amorphous structure of cellulose nanofibrils. In addition, the peak at  $1635\text{ cm}^{-1}$  belongs to the -OH bending of adsorbed water, because the water adsorbed in the cellulose molecules is too difficult to extract completely. The spectrum of (b) demonstrates that characteristic peaks of PLA correspond to the PLA molecular structure (Lalla and Chugh, 1990; Agarwal et al. 1998; Miyata and Masuko, 1998; Park et al. 1999). The stretching and bending peaks of the C=O appear at  $1761\text{ cm}^{-1}$  and  $1270\text{ cm}^{-1}$  respectively. The peaks at 2999, 2947, 1358, and  $1365\text{ cm}^{-1}$  are the asymmetric stretching, symmetric stretching, symmetric bending, and asymmetric bending. The peaks at 1192, 1134,  $1096\text{ cm}^{-1}$  are attributed to the C-O stretching. The bending of the -CH<sub>3</sub> is located at  $1457\text{ cm}^{-1}$ . The bending and stretching peaks of the -OH were apparent at  $1051\text{ cm}^{-1}$  and  $3512\text{ cm}^{-1}$ , respectively. And the peaks of  $925\text{ cm}^{-1}$  and  $870\text{ cm}^{-1}$  correspond to the stretching of the C-C single bond. Comparing the spectra Fig. 6d with Fig. 6c, the characteristic absorption peaks of the PLA/cellulose nanofibrils/PEG composites are nearly the same as those of PLA/cellulose nanofibrils composites. This is because the characteristic absorption peaks of the PEG are the same as those of the PLA and the cellulose nanofibrils. Otherwise, no new characteristic absorption peaks appeared in the spectra. This can be explained based on a hypothesis that cellulose nanofibrils are just combined with PLA and PEG by physical interactions without forming new functional groups.

With the addition of the cellulose nanofibrils, the C=O peak of PLA at  $1761\text{ cm}^{-1}$  became wider than that of the pure PLA. When the PEG was added, the C=O peak of the PLA/cellulose nanofibrils/PEG composites was wider than that of the PLA/cellulose nanofibrils composites, which indicates that the hydrogen bond forms between C=O of PLA and the -OH of cellulose nanofibrils. In the  $1250\text{-}1050\text{ cm}^{-1}$  region, the C-O stretching peaks of PLA /cellulose nanofibrils composites shifted slightly to a lower wavenumber, and the C-O stretching peaks of PLA/cellulose nanofibrils/PEG composites shifted markedly due to the addition of PEG. Hydrogen bonds can be also formed between the C-O of PLA and -OH of cellulose nanofibrils. This means that there exist intermolecular interactions in the PLA/cellulose nanofibrils composites; the PEG can improve the intermolecular interaction and then enhance the interfacial interaction between PLA and the cellulose nanofibrils. The C-O-C and the terminal -OH of the PEG can form hydrogen-bonding or dipolar interactions with PLA and cellulose nanofibrils respectively, which connect the PLA and the cellulose nanofibrils like a bridge.

## CONCLUSIONS

1. In summary, nanocomposites based on PLA and cellulose nanofibrils were prepared successfully. The mechanical properties of the composite were decreased by addition

of just the cellulose nanofibrils. Both tensile strength and the elongation rate were increased when the cellulose nanofibrils and PEG were added to the PLA matrix. The interfacial interaction or the compatibility between PLA and cellulose nanofibrils was improved by PEG.

2. A chemo-mechanical method was applied to make the cellulose nanofibrils disperse evenly in the organic solvent without the freeze-drying process. The mechanical properties of the nanocomposites, which depend strongly on PEG, were significantly improved by the incorporation of the cellulose nanofibrils and dispersing with the PEG (1000).
3. The cellulose nanofibrils dispersed evenly in the matrix when PEG was present. The interfacial contact between hydrophobic PLA and hydrophilic cellulose nanofibrils was improved significantly by adding the PEG to the PLA matrix.
4. The fracture surfaces of the three materials become more and more uneven with the addition of nanofibers and PEG to the PLA matrix. This was due to the interfacial adhesive force.
5. PEG can improve the intermolecular interaction and then enhance the interfacial interaction between PLA and the cellulose nanofibrils, because the C-O-C and the terminal O-H can form hydrogen-bonding or dipolar interactions between PLA and cellulose nanofibrils, which connects the PLA and the cellulose nanofibrils like a bridge.

## ACKNOWLEDGMENTS

We are thankful for the financial supports of the research from National Science Foundation of China (30871967) and Major State Basic Research Development Program of China (973 Program) (No. 2010CB732204) and State Forestry Administration (2008-4-075).

## REFERENCES CITED

- Agarwal, M., Koelling, K. W., and Chalmers, J. J. (1998). "Characterization of the degradation of polylactic acid polymer in a solid substrate environment," *Biotechnology Progress* 14(3), 517-526.
- Angles, M. N., and Dufresne, A. (2001). "Plasticized starch/tunicin whiskers nanocomposites materials," *Macromolecules* 34(9), 2921-2931.
- Asako, H., Masaki, T., and Fumitaka, H. (1997). "Culture conditions producing structure entities composed of cellulose I and II in bacterial cellulose," *Cellulose* 3, 239-245.
- Azizi, Samir, M. A., Alloin, F., and Dufresne, A. (2005). "Review of recent research into cellulosic whiskers, their properties and their application in nanocomposite field," *Biomacromolecules* 6(2), 612-626.
- Beck-Candanedo, S., Roman, M., and Gray, D. G. (2005). "Effect of reaction conditions on the properties and behavior of wood cellulose nanocrystal suspensions," *Biomacromolecules* 6(2), 1048-1054.

- Bondeson, D., Mathew, A., and Oksman, K. (2006). "Optimization of the isolation of nanocrystals from microcrystalline cellulose by acid hydrolysis," *Cellulose* 13, 171-180.
- Dai, Q. Z., and Kadla, J. F. (2009). "Effect of nanofillers on carboxymethyl cellulose/hydroxyethyl cellulose hydrogels," *Journal of Applied Polymer Science* 114(3), 1664-1669.
- Dubief, D., Samain, E., and Dufresne, A. (1999). "Polysaccharide microcrystals reinforced amorphous poly ( $\beta$ -hydroxy-octanoate) nanocomposite materials," *Macromolecules* 32(18), 5765-5771.
- Dufresne, A. (2000). "Dynamic mechanical analysis of the interphase in bacterial polyester/cellulose whiskers natural composites," *Composite Interfaces* 7(1), 53-67.
- Favier, V., Chanzy, H., and Cavaille, J. Y. (1995). "Polymer nanocomposites reinforced by cellulose whiskers," *Macromolecules* 28(18), 6365-6367.
- Gousse, C., Chanzy, H., Excoffier, G., Soubeyrand, L., and Fleury, E. (2002). "Stable suspensions of partially silylated cellulose whiskers dispersed in organic solvents," *Polymer* 43(9), 2645-2651.
- Gray, D. G., and Roman, M. (2006). "Cellulose nanocomposites," ACS Symposium series, American Chemical Society Oxford Press 938, 26-32.
- Gupta, B., and Revagade, N. (2007). "Poly (lactic acid) fiber: An overview," *Progress in Polymer Science* 32, 455-482.
- Heux, L., Chauve, G., and Bonini, C. (2000). "Nonflocculating and chiral-nematic self-ordering of cellulose microcrystals suspensions in nonpolar solvents," *Langmuir* 16(21), 8210-8212.
- Lalla, J. K., and Chugh, N. N. (1990). "Effects of morphology, conformation and configuration on the IR and Raman spectra of various poly(lactic acid)," *Indian Drugs* 27(10), 516-522.
- Lu, J., Askeland, P., and Drzal, L. T. (2008). "Surface modification of microfibrillated cellulose for epoxy composite applications," *Polymer* 49, 1285-1296.
- Lunt, J. (1998). "Large-scale production, properties and commercial applications of polylactic acid polymers," *Polymer Degradation and Stability* 59, 145-151.
- Mangiacapra, P., Gorrasi, G., Sorrentino, A., and Vittoria, V. (2005). "Biodegradable nanocomposites obtained by ball milling of pectin and montmorillonites," *Carbohydrate Polymers* 64, 516-523.
- Marras, S. I., Zuburtikudis, I., and Panayiotou, C. (2007). "Nanostructure vs. microstructure: Morphological and thermomechanical characterization of poly(L-lactic acid)/layered silicate hybrids," *European Polymer Journal* 43, 2191-2206.
- Miyata, T., and Masuko, T. (1998). "Crystallization behaviour of poly(l-lactide)," *Polymer* 39, 5515-5521.
- Nada, A. M. A., El-Kady, M. Y., Abd El-Sayed, E. S., and Amine, F. M. (2009). "Preparation and characterization of microcrystalline cellulose (MCC)," *BioResources* 4(4), 1359-1371.
- Oksman, K., Mathew, A. P., Bondeson, D., and Kvien, I. (2006). "Manufacturing process of cellulose whiskers/polylactic acid nanocomposites," *Composites Science and Technology* 66, 2776-2784.

- Park, J. W., Lee, D. J., and Yoo, E. S. (1999). "Melt theology of poly(lactic acid): Consequences of blending chain architectures," *Korea Polymer Journal* 7(2), 93-101.
- Peng, S. W., Wang, X. Y., and Dong, L. S. (2005). "Special interaction between poly(propylene carbonate) and corn starch," *Polymer Composites* 26, 37-41.
- Petersson, L., Kvien, I., and Oksman, K. (2007). "Structure and thermal properties of poly(lactic acid)/cellulose whiskers nanocomposite materials," *Composites Science and Technology* 67, 2535-2544.
- Salmi, J., Nypelo, T., Osterberg, M., and Laine J. (2009). "Layer structures formed by silica nanoparticles and cellulose nanofibrils with cationic polyacrylamide (C-PAM) on cellulose surface and their influence on interactions," *BioResources* 4(2), 602-625.
- Samir, M. A. S. A., Alloin, F., Sanchez, J. Y., and Dufresne, A. (2004). "Cross-linked nanocomposite polymer electrolytes reinforced with cellulose whiskers," *Macromolecules* 37(13), 4839-4844.
- Singha, A.S., and Thakur, V.K. (2009). "Study of mechanical properties of urea-formaldehyde thermosets reinforced by pine needle powder," *BioResources* 4(1), 292-308.
- Sturcova, A., Davies, G. R., and Eichhorn S. J. (2005). "Elastic modulus and stress-transfer properties of tunicate cellulose whiskers," *Biomacromolecules* 6(2), 1055-1061.
- Takahashi, N., Okubo, K. and Fujii, T. (2005). "Development of green composite using microfibrillated," Cellulose extracted from bamboo," *Bamboo Journal* 22, 81-92.
- Thomas, S., Pothan, L. A., and Cherian, B. M. (2009). "Advances in natural fibre reinforced polymer composites: macro to nanoscales," *International Journal of Materials and Product Technology* 36(1-4), 317-333.
- Wu, C. S. (2008). "Characterizing biodegradation of PLA and PLA-g-AA/starch films using a phosphate-solubilizing bacillus species," *Macromolecular Bioscience* 8, 560-567.
- Wu, C. S., and Liao, H. T. (2005). "A new biodegradable blends prepared from polylactide and hyaluronic acid," *Polymer* 46, 10017-10026.
- Yang, J. H., Yu, J. G., Feng, Y., and Ma, X. F. (2006). "Study on the properties of ethylenebisformamide plasticized corn starch (EPTPS) with various original water contents of corn starch," *Carbohydrate Polymers* 69, 256-261.
- Zhang, G. B., Zhang, J. M., Zhou, X. S., and Shen, D. Y. (2003). "Miscibility and phase structure of binary blends of polylactide and poly (vinylpyrrolidone)," *Journal of Applied Polymer Science* 88, 973-979.

Article submitted: April 26, 2010; Peer review completed: June 7, 2010; Revised version received: June 24, 2010; Accepted: June 26, 2010; Published: June 28, 2010.